Int. J. Exp. Path. (2007), 88, 257–270
doi: 10.1111/j.1365-2613.2007.00532.x

ORIGINAL ARTICLE

Investigation of intratumoural and peritumoural lymphatics expressed by podoplanin and LYVE-1 in the hybridoma-induced tumours

R.C. Ji*, Y. Eshita† and S. Kato*

*Department of Anatomy, Biology and Medicine and †Department of Infectious Diseases, Oita University Faculty of Medicine, Oita, Japan

INTERNATIONAL JOURNAL OF EXPERIMENTAL PATHOLOGY

Summary

Tumour-associated lymphatics contribute to a key component of metastatic spread, however, the biological interaction of tumour cells with intratumoural and peritumoural lymphatics (ITLs and PTLs) has remained unclear. To address this important issue, we have focused on the morphological and molecular aspects of newly formed lymphatics (lymphangiogenesis) and pre-existing lymphatics in the intratumoural and peritumoural tissues by using a hybridoma-induced tumour model. In the present study, ITLs with very high vessel density within the tumour mass showed small and flattened contours that varied from non-solid-to-solid tumours, whereas PTLs were relatively disorganized and tortuous, and packed with a cluster of tumour cells at the tumour periphery. Lymphatic endothelial cells (LECs) both in ITLs and PTLs were expressed with LYVE-1 and podoplanin in various tumour tissues, in which initial lymphatics were extremely extended and dilated. The tumour cells were frequently detected adhering to or penetrating lymphatic walls, especially near the open junctions. In the metastatic tissues, lymphangiogenic vasculatures occurred within the tumour matrix, and collecting PTLs represented abnormal twisty valve leaflets. The Western blot and RT-PCR analysis showed local variations of LEC proliferating potentials and lymphatic involvement in metastasis by a distinct profile of the protein and mRNA expression by LYVE-1, podoplanin, *Prox-1* and vascular endothelial growth factor-3 (VEGFR-3). These findings indicated that both ITLs and PTLs, including enlarged pre-existing and newly formed lymphatics, may play a crucial role in metastasis with an active tumour cell adhesion, invasion, migration and implantation.

Keywords

intratumoural lymphatics, lymphatic endothelial cell, LYVE-1, peritumoural lymphatics, podoplanin, *Prox-1*, tumour metastasis, VEGFR-3

Received for publication:
29 January 2007
Accepted for publication:
18 March 2007

Correspondence:
Rui-Cheng Ji, MD PhD
Department of Anatomy, Biology and Medicine
Oita University Faculty of Medicine
Oita 879-5593
Japan
Tel. & Fax: +81 097 586 5623
E-mail: ji@med.oita-u.ac.jp

The lymphatics are involved in many biological processes, such as the regulation of permeability and active contractility for the return of extravasated fluid, proteins and macromolecules from the tissue space to the bloodstream. Recently, a great advance in the lymphology and oncology has been made with the identification of the lymphatic endothelial cell (LEC)-specific markers, such as the receptor of the vascular endothelial growth factor (VEGFR-3), the lymphatic vessel endothelial hyaluronan receptor-1 (LYVE-1), the transcription prospero-related homeobox gene (*Prox-1*), the integral plasma membrane glycoprotein of podocytes (podoplanin), and the O-linked sialoglycoprotein D2-40 (Kahn *et al.* 2002; Alitalo *et al.* 2005; Ji 2006a). Notably, podoplanin and D2-40 are also useful markers for the diagnosis of a subset of angiosarcoma, seminomas, epithelioid mesothelioma and hemangioblastoma (Breiteneder-Geleff *et al.* 1999; Ordonez 2005; Roy *et al.* 2005). Therefore, growing recognition of the multiple functions of these LEC-specific markers for important physiological and pathological events may be helpful in identifying the crucial changes in tumour tissues subjected to lymph circulation and ultimately in the search for rational therapeutic approaches.

Experimental evidences have suggested a significant correlation between VEGF-C/-D (the ligands of VEGFR-3) expression, tumour lymphangiogenesis and formation of metastasis in regional lymph nodes (Skobe *et al.* 2001; Stacker *et al.* 2001), however, the expression of lymphangiogenic factors is inconsistent with nodal metastasis in human tumours. In previous clinical studies, no correlation was indicated between lymphangiogenesis and any tumour parameter in hepatocellular carcinoma (Mouta Carreira *et al.* 2001), and even no information was provided about lymphangiogenesis in breast cancer (Williams *et al.* 2003). Of note, in spite of the occurrence of widespread lymphangiogenesis in cancers like head and neck squamous cell carcinomas (Beasley *et al.* 2002) and cutaneous melanomas (Dadras *et al.* 2003), the degree of lymphangiogenesis alone is not an independent prognostic factor for these tumours. It might reflect the fact that tumour lymphangiogenesis and lymphatic metastasis are complex mechanisms that can differ significantly in tumours of different types or anatomical locations.

Despite the continuing accumulation of correlative basic and clinical data, the biological significance of LECs, especially the interaction of lymphatic localization and morphology with tumour cells has yet to be fully demonstrated. Two essentially conflicting views maintain in the dissemination of tumour cells from the primary site. Some are of the opinion that tumours metastasize solely by the invasion of pre-existing lymphatics at the tumour periphery due to the intratumoural high pressures, while others onsider that tumours metastasize by promoting newly formed lymphatics within the tumour parenchyma (Alitalo & Carmeliet 2002; Achen *et al.* 2005; Ji 2005, 2006a). Therefore, several questions on tumour lymphatic metastasis still remain unsettled, (a) how tumour cells migrate and invade the lymphatic endothelial wall?; (b) which of the intratumoural or peritumoural lymphangiogenesis is a decisive factor for tumour metastasis?; and (c) what are the phenotypical and functional differences in pre-existing or newly formed lymphatics? Functionally, increased lymphatic permeability and interstitial changes of the tissue fluid pressure and flow may also form a prerequisite for the metastatic spread (Jussila *et al.* 1998). In this context, the present investigation was concentrated on the biological characteristics of LECs by using a multiple-organ tumour model to illustrate the importance of intratumoural lymphatics (ITLs) and peritumoural lymphatics (PTLs) in tumour metastasis.

Materials and methods

Production of hybridoma-induced tumour models

BALA/c mice, 5–8 weeks of age, were treated with 0.5 ml pristane (2,6,10,14-tetramethylpentadecane; Sigma, St Louis, MO, USA). And 5′-nucleotidase (5′-Nase) monoclonal antibody (JC815)-producing hybridoma cells were cultured in RPMI-1640 medium with L-glutamine and $NaHCO_3$ (Sigma) supplemented with 10% heat-inactivated foetal bovine serum (GibcoBRL, Grand Island, NY, USA), 100 IU/ml penicillin and 100μg/ml streptomycin (Flow Lab, Irvine, UK) at 37 °C in a humidified incubator with air and 5% CO_2 (Ji *et al.* 2003). After 3 weeks for pristane treatment, 10^6–10^7 hybridoma supernatant in the 0.5 ml culture medium was injected intraperitoneally. The booster was administrated in 2–4 weeks later. The ascites tumour fluid was removed in time from the abdominal cavity. The tumour-involved tissues including pancreas, diaphragm, intestine, liver, stomach, colon, kidney, urinary bladder, uterus, abdominal skin and abdominal and mediastinal lymph nodes were examined in 6–12 weeks of the first hybridoma injection. The experiment was approved by the Animal Research Ethics Committee of Oita University Faculty of Medicine.

Enzyme histochemistry

Samples were processed for 4% paraformaldehyde fixation in 0.1 M cacodylate buffer (pH 7.2), or directly snap-frozen in liquid nitrogen. Successive 5–7 μm cryosections were air-dried or treated in the same fixation.

Moreover, 5′-Nase activity for demonstrating lymphatics was conducted in the standard medium in addition to 2 mM *L*-tetramisole for 40–50 min at 37 °C. The lead-based medium contained 2.9 mM adenosine 5′-monophosphate (AMP; Sigma) and 3.6 mM $Pb(NO_3)_2$. Samples were immersed in 1% ammonium sulphide solution for 1–2 min at room temperature and then examined under a light microscope. For transmission electron microscopic (TEM) analyses, the ultrathin sections were stained with the cerium-based medium containing 1 mM AMP and 2 mM $CeCl_3$ for 30–40 min at 37 °C. The ALPase activity of the blood vessels was identified in tissue sections for 20–30 min at 4 °C by using the reaction medium of naphthol AS-MX phosphate and fast blue BB salt. For controls, the substrates were omitted from the above-mentioned mediums.

Immunohistochemistry

Serial cryosections fixed in 4% paraformaldehyde or paraffin sections fixed with 10% neutral formalin in 0.1 M phosphate-buffered saline (PBS, pH 7.4) were soaked in 0.3% hydrogen peroxide and 10% blocking serum [normal goat serum (NGS) or normal rabbit serum (NRS)]. Sections were incubated with VEGF-C (goat anti-human IgG, 1:200, Santa Cruz Biotechnology, Inc., Santa Cruz, CA, USA), VEGFR-3 (rabbit anti-mouse FLT-4 serum, 1:100, Alpha Diagnostic International, Co., San Antonio, TX, USA), podoplanin (hamster anti-mouse IgG, 1:200, AngioBio Co., Del Mar, CA, USA), *Prox-1* (rabbit anti-mouse serum, 1:500, AngioBio Co.), LYVE-1 (rabbit anti-mouse IgG, 1:100, RELIA*Tech* GmbH, Braunschwer, Germany), JC815 (5′-NasemAb, IgG, 1:400–1:800), CD31 (rat anti-mouse PECAM-1 IgG, 1:400, Cymbus Biotechnology Ltd, Hants, UK), vWF (rabbit anti-human von Willebrand factor IgG, 1:300, Dako, Glostrup, Denmark) for 60 min at room temperature or overnight at 4 °C. The subsequent incubation in biotinylated goat anti-rabbit IgG, rabbit anti-goat IgG, or goat anti-hamster IgG diluted to 1:100–200 was followed by treatment with streptavidin-biotinylated peroxidase complexes (Nichirei Corp., Tokyo, Japan). The peroxidase was visualized by incubation with 0.03% 3,3′-diaminobenzidine tetrahydrochloride (DAB) solution in 0.05 M Tris-HCl (pH 7.4). Sections were lightly counterstained with 1% methyl green or Mayer haematoxylin, and examined by light microscopy. Negative controls were done by using a non-immune serum or by omitting the primary antibodies.

The antigen sites of VEGFR-3, podopalnin, *Prox-1* and JC815 were further examined in ultrathin sections (85–90 nm) by a postembedding immunogold staining method. Fixed samples were dehydrated in a graded ethanol series at 4 °C, with a 1:1 LR White: 100% ethanol mixture for 1 h before being transferred to 100% LR White for 1 h with two changes. Tissues were then embedded in LR White by using a gelatin capsule. The resin was polymerized at 60 °C for 24 h. LR White sections mounted on Formvar-coated nickel grids were preincubated for 5 min face down on drops of buffer containing 0.1% bovine serum albumin (BSA) and transferred to a drop of 10% NGS or NRS in rinsing buffer for 15 min. Sections were then incubated on a drop of podopalnin, VEGFR-3, *Prox-1* and JC815. Sections for podoplanin immunohistochemistry were further incubated with goat anti-hamster IgG. Unbound primary or secondary antibody was then rinsed off the grids by buffer, and incubation was continued with goat anti-rabbit IgG, rabbit anti-goat IgG and goat anti-mouse IgG bound to 5 nm gold particles (Auroprobe EM-GAR G5; Janssen Pharmaceutica, Beerse, Belgium) in a 1:70 dilution. Silver enhancement was performed in some samples after being rinsed to remove excess unbound gold particles. The sections were counterstained for 3–6 min with diluted aqueous uranyl acetate and lead citrate, and examined with a JEM 1200EX II electron microscope.

SDS-PAGE and Western blot analyses

Samples of fresh tumour-involved tissues were homogenized in lysis buffer (50 mM Tris-HCl, 150 mM NaCl, 0.02% sodium azide, 50μg/ml phenylmethysulphonyl fluoride, 2μg/ml aprotinin, 2μg/ml leupeptin, 2μg/ml pepstatin A, 1% Igepal CA-630). The homogenate was subjected to centrifugation at 12,000 ***g*** for 10 min at 4 °C. The supernatant was collected and used for protein determination using Bio-Rad protein assay kit (Bio-Rad, Richmond, CA, USA). Protein samples for SDS polyacrylamide-gel electrophoresis (SDS-PAGE) were homogenized directly into 10% vol/wt of SDS sample buffer (125 mM Tris-HCl, pH 6.8, with 2% SDS, 10% glycerol, 5%β-mercaptoethanol, and 1.25×10^{-5} bromophenol blue). All SDS samples were heated to 100 °C for 5 min and then clarified at 3000 g for 5 min. As much as 15μl SDS sample buffer was applied per slot and electrophoresed on slab gels (6 cm wide, 10 cm long, 1.5 mm thick) in the presence of 0.1% SDS with a 10% separating gel and a 4.75% stacking gel at 170 v for 55 min. Resolved proteins were treated with Coomassie brilliant blue R250 for visualization and preservation, or directly transferred to immunoblotting.

Immunoblotting was performed immediately upon the completion of the SDS-PAGE. The separated proteins were transferred onto a nitrocellulose membrane using the transfer buffer (39 mM glycine, 48 mM Tris-HCl, pH 8.3,

0.037% SDS, 20% methanol) at 100 v for 3 h. The sheets were washed in 0.1% Tween 20/0.1 M PBS (T-PBS, pH 7.4) for 10 min. Before immunostaining, 2% Ponceau S, a reversible binding solution, was used for localization of antigens. The trimmed sheets were blocked with 3% BSA-PBS for 15 min, and incubated with VEGFR-3 diluted 1:500–1000 in 0.1% T-PBS for 60 min at room temperature. The subsequent incubations were undertaken in biotinylated goat anti-rabbit IgG and streptavidin-biotinylated peroxidase reagent for each 50 min. DAB development of the sheets was stopped with a water rinse followed by air drying.

Reverse transcription-polymerase chain reaction analysis

The mRNA expressions of VEGFR-3, podoplanin, *Prox-1*, LYVE-1 and vWF in fresh tumour-involved tissues were evaluated by semi-quantitative reverse transcription-polymerase chain reaction (RT-PCR) (Mancardi *et al.* 1999; Burke & Oliver 2002; Schiwek *et al.* 2004; Morisada *et al.* 2005). Total RNAs were extracted using Rneasy Mini Kit reagent (Qiagen Inc., Valencia, CA, USA). First strand complementary DNA was prepared from RNA template (1μg) using oligo (dT) specific sets of primers and Qiagen one step RT-PCR kit. The RT-reaction profile was 50 °C for 30 min, followed by 95 °C for 15 min. The amplification procedure was performed by 35 cycles, denaturalizing at 94 °C for 30 s, annealing at 57 °C for 1 min, and extending at 72 °C for 1 min and 45 s. For each amplification reaction, the specific negative control (amplification of a sample containing the same reagents except reverse transcriptase) was included. The sequences of primers are as follows: VEGFR-3 (788 bp) forward and reverse, 5′-TTG GCA TCA ATA AAG GCA G-3′ and 5′-CTG CGT GGT GTA CAC CTT A-3′; vWF (360 bp) forward and reverse, 5′-TGG TCC GCT ATG TCC AAG GT-3′ and 5′-TCT TAT TGA AGT TGG CTT CA-3′; LYVE-1 (418 bp) forward and reverse, 5′-TTC CTC GCC TCT ATT TGG AC-3′ and 5′-ACG GGG TAA AAT GTG GTA AC-3′; *Prox-1* (674 bp) forward and reverse, 5′-GTG TGC AGA TGC CTA GTT CCA CA-3′ and 5′-TAC TGG TGA CTC CAT CAT TGA TG-3′; podoplanin (799 bp) forward and reverse, 5′-TGG AGG GCT TAA TGA ATC TA-3′ and 5′-GGG CTG GAA TGT GTA TGT AT-3′; the glyceraldehyde-3-phosphate dehydrogenase (GAPDH, 710 bp) (GenBank accession no. NM_008084) forward and reverse, 5′-GTG AAG GTC GGT GTG AAC GGA TTT G-3′ and 5′-ACA TTG GGG GTA GGA ACA CGG AAG G-3′. All these primers were confirmed to yield the expected products under these conditions. The PCR products were electrophoresed on 1.5% agarose gels and detected by ethidium bromide staining.

Computer-assisted morphometric lymphatic analysis

LYVE-1 or/and podoplanin stained sections were examined by two independent investigators using an Olympus BX50 microscope (objective lens ×20, field of view, 0.3104 mm^2) and digital images of tumour-associated lymphatics were captured using a SPOT digital camera. For each tumour section, three fields with the highest lymphatic vessel density (hot spots) were identified at the tumour periphery and within the tumour mass. Morphometric analyses of the digital images were performed using the NIH IMAGE 1.62 software (National Institutes of Health, Bethesda, MD, USA) to determine the lymphatic vessel density, defined as the number of lymphatics per mm^2, the average lymphatic size, and the area fraction of lymphatics (%) that is the area of lymphatics per unit area of tissues.

Statistical analyses

The evaluation of the lymphatic vessel density, average size and area fraction in the intratumoural and peritumoural tissues was made by one-way analysis of variance (ANOVA) followed by Tukey and Bonferroni *post hoc* tests using SYSTAT 11 (SYSTAT Software Inc., Point Richmond, CA, USA). Differences were considered statistically significant for *P*-values less than or equal to 0.05.

Results

Lymphatic size, lymphatic vessel density and lymphatic area fraction in intratumoural and peritumoural tissues

In the mouse model, hybridoma cells frequently invaded the abdominal organs, especially the pancreas, the diaphragm and the intestine. The lymphatic size of the normal tissues was smaller than that of peritumoural tissues ($P < 0.05$, $n = 999$), but much larger than intratumoural tissues ($P < 0.001$, $n = 1390$). The lymphatic size showed a great difference in intratumoural and peritumoural tissues ($P < 0.001$) (Figure 1a). Lymphatic vessel density, mean lymphatic counts per millimetre squared, was significantly higher in the intratumoural than peritumoural tissues ($P < 0.001$, $n = 69$) (Figure 1b). Lymphatic area fraction, a ratio of total lymphatic area to total area within a view field, was increased in intratumoural ($P < 0.001$, $n = 76$) and peritumoural ($P < 0.001$, $n = 131$), compared with normal tissues (Figure 1c). Scattered cell clusters were features of non-solid tumour growth. In comparison with the solid tumour mass, the lymphatics represented an enlarged size in non-solid tumour tissues ($P < 0.001$, $n = 1641$) (Figure 1d).

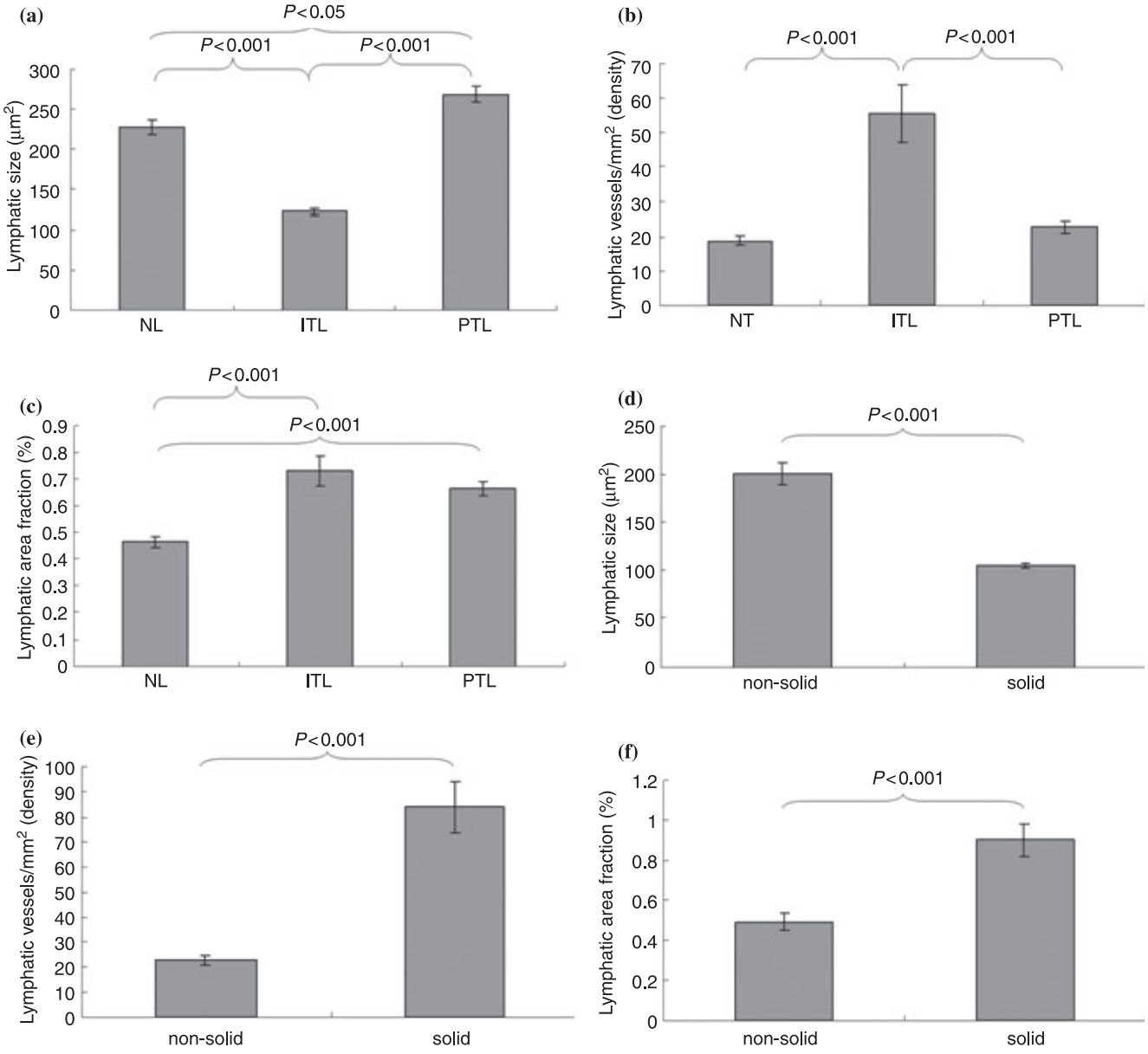

Figure 1 In the hybridoma-induced mouse model, the lymphatic size (μm^2, a and d), lymphatic vessel density (counts/mm^2, b and e), and lymphatic area fraction (%, c and f) show significant differences between the intratumoural and peritumoural tissues, and between non-solid and solid tumour tissues.

Lymphatic vessel density ($n = 25$) and area fraction ($n = 76$) were significantly higher in the solid tumour mass than in the non-solid tumour tissue ($P < 0.001$) (Figure 1e,f).

Histochemistry and morphology of intratumoural and peritumoural lymphatic vessels

Immunohistochemical localization of the antigens recognized by VEGFR-3, LYVE-1, podoplanin, *Prox-1* and JC815, and 5′-Nase enzyme activity were examined in the lymphatics of the small intestine, stomach, diaphragm, skin, pancreas, liver and other tumour tissues. In the mucosa and submucosa of the stomach, 5′-Nase-positive lymphatics showed weaker CD31 immunoactivity than ALPase-positive blood vessels, and expressed VEGFR-3 rather than VEGF-C (Figure 2a–d). In the pancreatic tumour tissues, 5′-Nase-positive lymphatics were distributed at the tumour periphery, and clustered within the tumour tissues where the

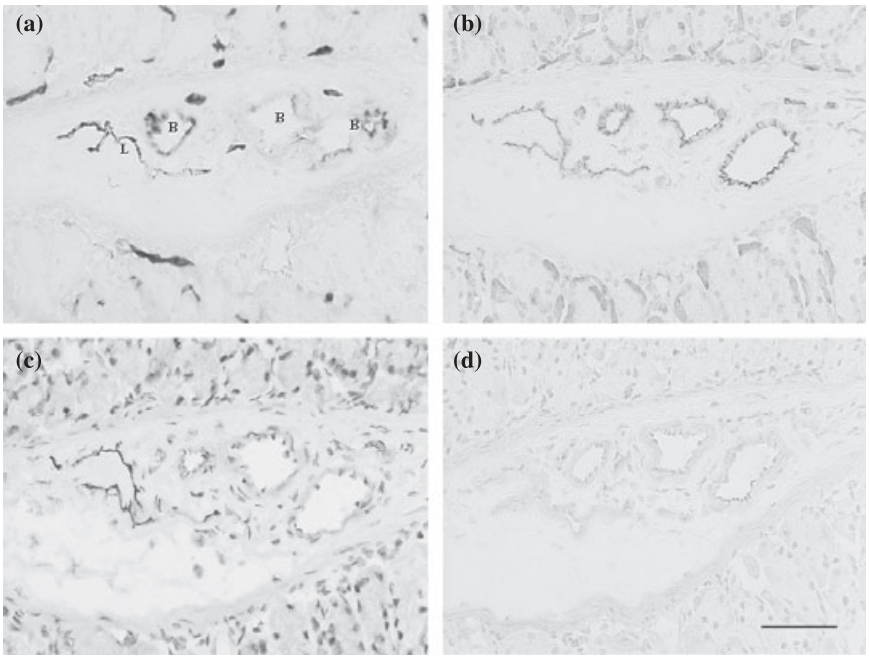

Figure 2 Photomicrographs of the hybridoma-induced tumour model. In serial cryosections of the stomach, 5′-Nase-positive lymphatics in the mucosa and submucosa show flattened and irregular contour, in comparison with ALPase-positive blood vessels (a). The lymphatics represent weaker CD31 immunoreactivity than the blood vessels (b), and strongly express VEGFR-3 (c) but not VEGF-C (d). L, lymphatic vessel; B, blood vessel. Bars = 50μm.

tumour cells with strong ALPase activity were compactly arranged. ITLs were quite small, flattened or irregular, and occasionally filled with tumour cells in the lumen (Figure 3a). The numerous podoplanin-expressing lymphatics extended into intralobular pancreatic parenchyma immediately near the blood vessels and ducts (Figure 3b). PTLs were relatively enlarged and disorganized, and packed with a cluster of tumour cells at the tumour periphery. The lymphatic wall seemed to be extremely extended and dilated (Figure 3c). *Prox-1* was not only expressed in enlarged PTLs, but also up-regulated in blood vessels in the boundary zone between uterine and tumour tissues (Figure 3d). In the hepatic tumour, podoplanin was specifically expressed in the lymphatics that had a thin endothelial wall and irregular contour, and in the tumour cells adjacent to the hepatic tissues (Figure 3e). In the hepatic capsule, ITLs expressed for podoplanin did not show collapsed shape in the extracellular space where low tumour cell density contrasted with the loose connective matrix, and the scattered tumour cells easily passed through the slender endothelial walls (Figure 3f). LYVE-1-expressing PTLs and ITLs were filled with a great number of tumour cells, in which ITLs showed a clear outline shape within the tumour tissues (Figure 3g,h). PTLs stained with 5′-Nase were relatively tortuous and clustered and LYVE-1-expressing double lymphatic layers were obviously enlarged in the intestine-tumour boundary zone (Figure 3i,j). Tumour cells were significantly expressed for VEGF-C and *Prox-1* (Figure 4a,b). In the metastatic lymph node, the high-endothelial venule showed strong vWF immunoreactivity (Figure 4c). Tumour cells were filled the medullary sinus, whereas podoplanin-expressing cells were seen within the medullary cords (Figure 4d). The metastasis was much more seen in the abdominal lymph nodes than thoracic lymph nodes.

In the TEM, dense 5′-Nase-cerium precipitates were evenly distributed on the luminal and abluminal surfaces of lymphatics and on the surface of valves, and extended into typical interdigitating junctions (Figures 5 and 6). The initial lymphatics became collapsed due to the squeeze of the malignant cells within the tumour tissues or extremely enlarged due to obstruction of tumour cell emboli at the tumour periphery (Figure 5a,b). Collecting lymphatics showed typical two-flap valves in the pancreas without significant invasion of tumour cells, and disordered twisty valves in the abdominal skin involved by severe metastasis (Figure 5c,d). The open junction was often seen adjacent to tumour cells in the initial lymphatics (Figure 5e). Within tumour tissues, lymphatic-like structures were attached with 5′-Nase reaction product on the incomplete luminal surface (Figure 5f). The tumour cells with their metabolic products adhered to or penetrated slender lymphatic walls in various patterns (Figure 6). In the immunogold TEM, *Prox-1* was mainly expressed as a granular product in the nucleus of LECs (Figure 7a). Immunoreactivities of podoplanin, JC815 and VEGFR-3 were detected on the endothelial surfaces and valve tips (Figure 7b–d). The podoplanin-positive cell was distinctly deposited with the reaction particulate in the organelles (Figure 7e).

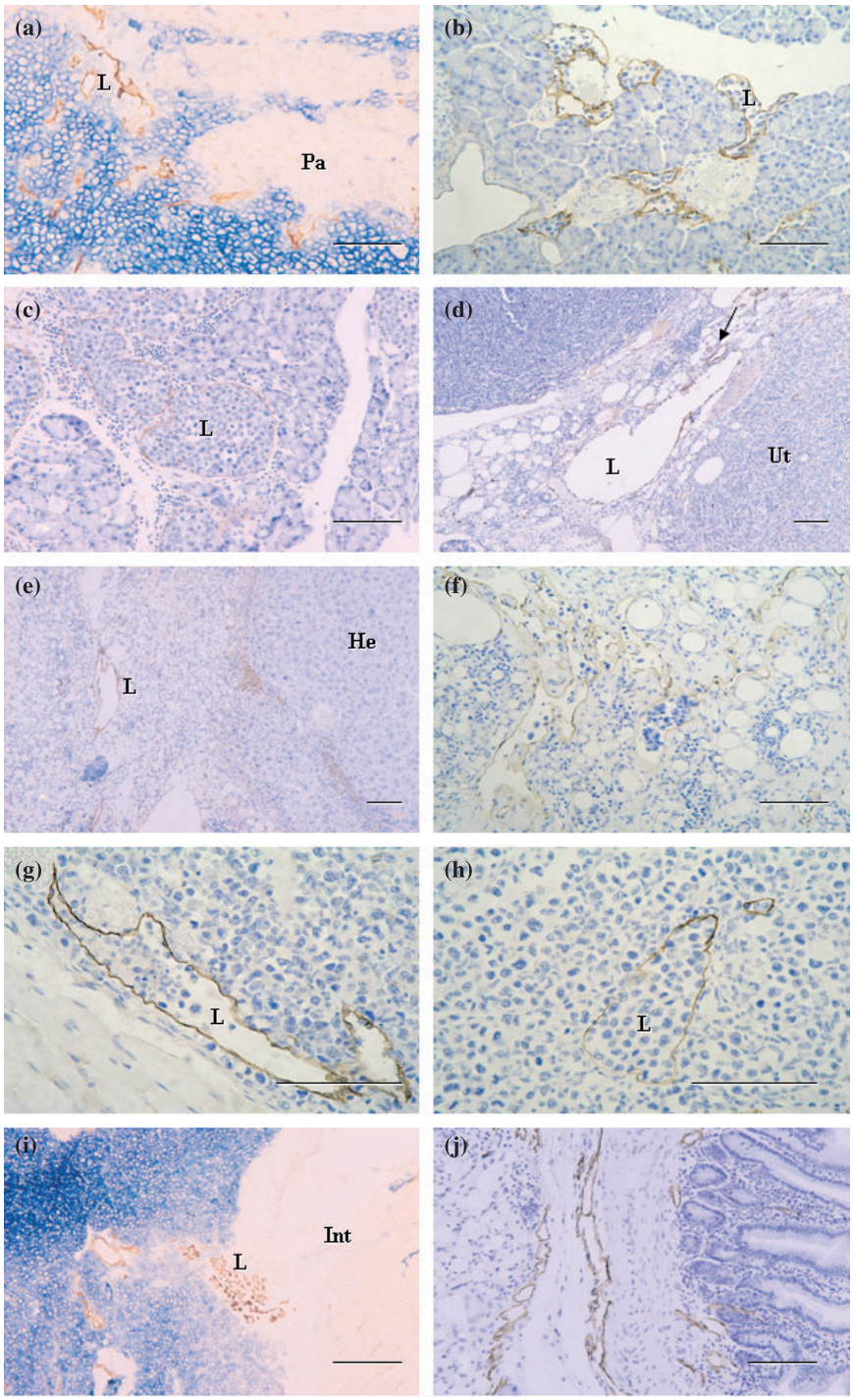

Figure 3 Photomicrographs of the sections through hybridoma-induced-tumour tissues. (a–c) 5′-Nase-positive intratumoural lymphatics (ITLs) and peritumoural lymphatics (PTLs) are obviously clustered within the tumour mass that show very strong ALPase activity or distributed in the pancreas (Pa)-tumour boundary zone (a). The numerous podoplanin-expressing lymphatics filled with a cluster of tumour cells, extend into the pancreatic parenchyma (b), and PTLs expressed for podoplanin are extremely enlarged due to squeeze of tumour cells (c). (d) *Prox-1* is expressed by the enlarged lymphatics, and up-expressed by the blood vessels (arrow) in the tumour–uterus (Ut) boundary zone. (e) Podoplanin is specifically expressed in the lymphatic vessel with a thin endothelial wall and irregular contour, and in some tumour cells adjacent to the hepatic tissues (He). (f) In the hepatic capsule, ITLs expressed for podoplanin show different sizes due to the low density of tumour cells and loose intratumoural matrix, in which some lymphatics are filled with tumour cells. (g and h) In the skin, tumour cells are accumulated in both LYVE-1-expressing peritumoural (g) and intratumoural (h) lymphatics. ITLs show uncollapsed although the tumour tissue appears a high-density mass (h). (i and j) In the intestine (Int)-tumour boundary zone, 5′-Nase-positive ITLs are small and flattened, and PTLs are accumulated in the tumour periphery (i), and the lymphatics with LYVE-1 immunoreactivity become obviously enlarged (j). L, lymphatic vessel. Bars = 100μm.

Expression of lymphatic endothelial markers in tumour tissues

In the Western blot, specific detection of VEGFR-3 was analysed in the tumour tissues of pancreas, diaphragm, intestine, skin, uterus, colon, liver, kidney and lymph node. The blotting sheet transferred from the SDS-PAGE gels was immunohistochemically stained with VEGFR-3 by indirect peroxidase method. The positive reacted bands of VEGFR-3 on the nitrocellulose strip were noted at

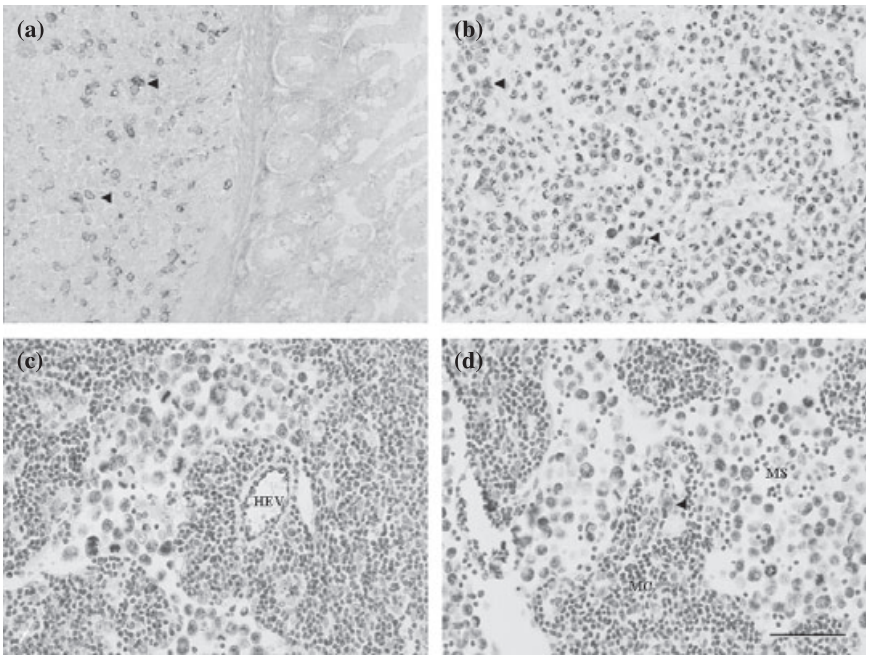

Figure 4 Expression of VEGF-C (a), *Prox-1* (b), vWF (c) and podoplanin (d) in lymphatics and tumour cells. (a) VEGF-C-expressing tumour cells (arrowheads) are located near the intestinal muscular layer. (b) Numerous *Prox-1*-expressing cells (arrowheads) are clearly defined within the tumour tissues. (c, d) In the metastatic lymph node, a high-endothelial venule (HEV) shows strong vWF immunoreactivity (c), and a podoplanin-expressing cell (arrowhead) is seen within the medullary cords (MC) (d), whereas the medullary sinus (MS) contains a cluster of tumour cells (c, d). Bars = 50μm.

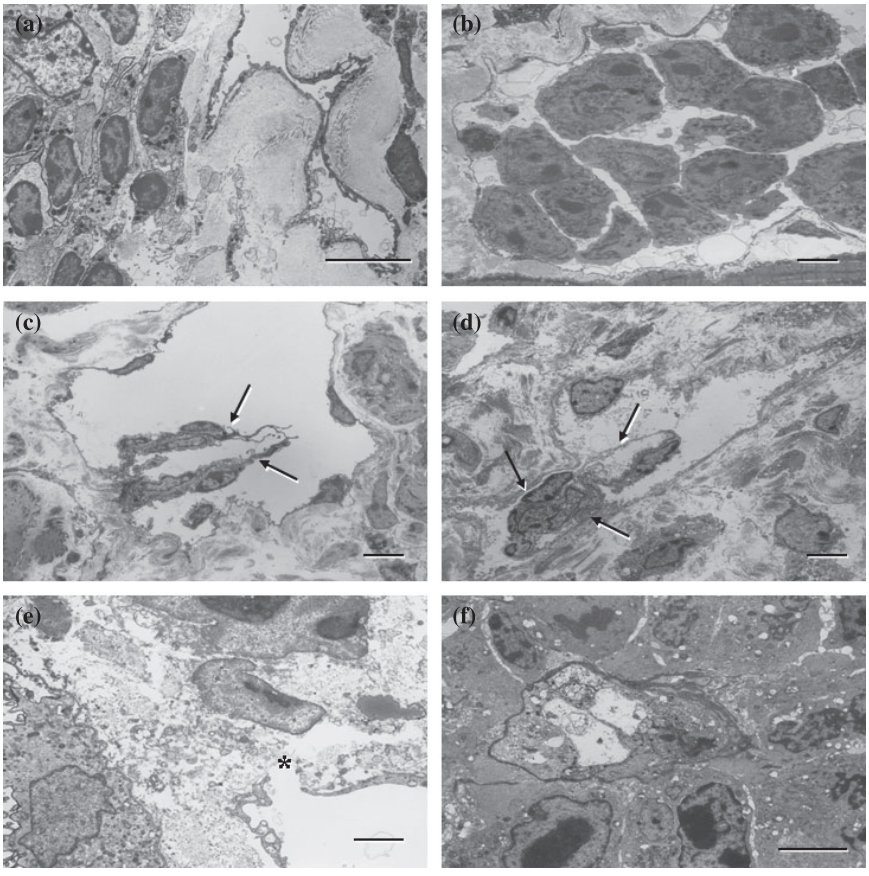

Figure 5 Transmission electron microscopic (TEM) views of 5′-Nase-positive lymphatics. Dense 5′-Nase-cerium precipitates are evenly distributed on the luminal and abluminal surfaces of the endothelial cells, and on the surface of the valves. (a and b) In the pancreas-tumour boundary zone, the lymphatics become collapsed (a, intratumoural) or enlarged (b, peritumoural) due to squeezing or over-filling of crowded tumour cells in the diaphragm. (c and d) The collecting lymphatic vessel shows typical two-flap valves (arrows) in the pancreas (c) and abnormally twisty valves (arrows) in the abdominal skin (d). (e and f) The open junction (asterisk) in the initial lymphatics of intestinal walls is adjacent to tumour cells (e). Within tumour tissues of the skin, the lymphatic-like structure is attached with 5′-Nase-cerium product on its incomplete luminal surface (f). (a–d, f) bars = 5μm; (e) bar = 2μm.

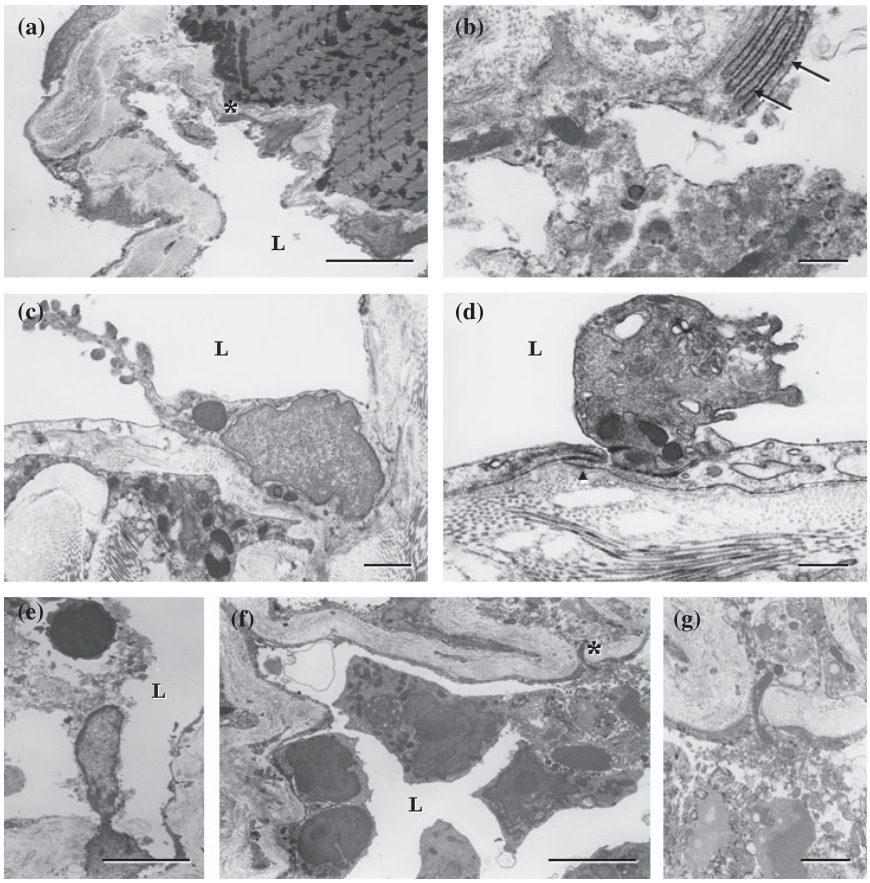

Figure 6 The tumour cells and their metabolic products stick to or penetrate 5′-Nase-positive lymphatic walls, especially near the intercellular junctions in the diaphragm. Panels (b) and (g) are further magnification of the area indicated by the asterisks of (a) and (f) respectively. Dense 5′-Nase-cerium precipitates extend into the typical interdigitating (b, arrows) and overlapping (d, arrowhead) junctions. L, lymphatic vessel. a, e, f, bars = 5μm; c, g, bars = 1μm; b,d, bars = 0.5μm.

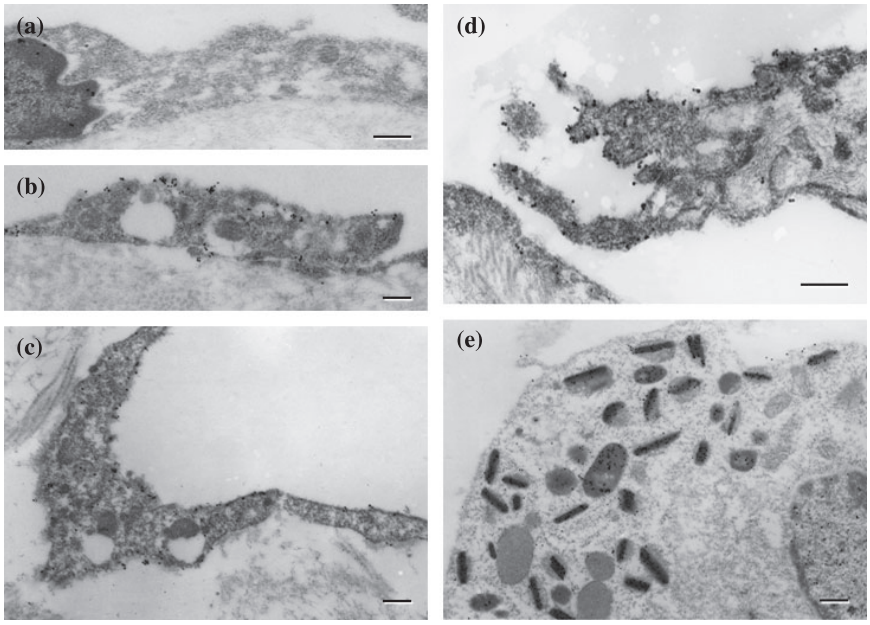

Figure 7 Immunocytochemistry on the lymphatic endothelial cells (LECs) (a–d) and tumour cell (e). (a) *Prox-1*-expressing lymphatic vessel in the intestine shows a nuclear deposition of the product. (b)–(d) LECs in the diaphragm display immunoreactivities for podoplanin (b), JC815 (c) and VEGFR-3 (d), which are mainly detected as a granular deposition on cell surfaces (b, c) and valve tips (d). (e) The podoplanin-positive cell is distinctly deposited with reaction product in the organelles in intestine-tumour boundary tissues. Bars = 0.2μm.

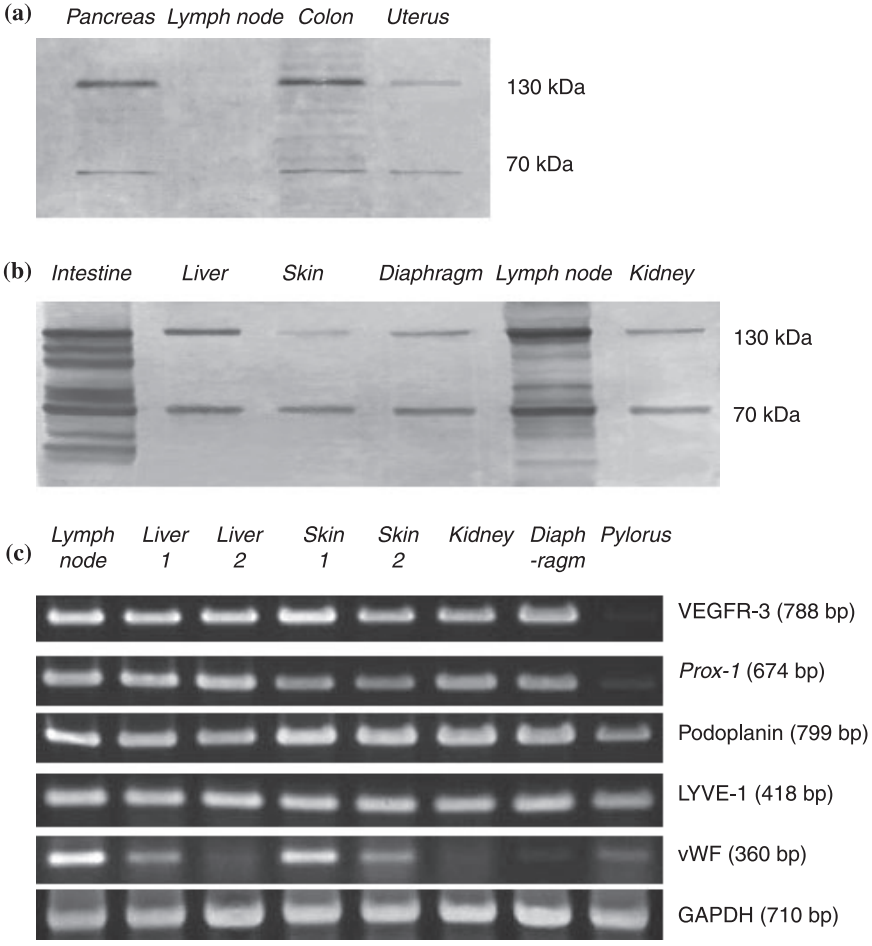

Figure 8 Western blot (a, b) and RT-PCR (c) analysis in hybridoma-induced tumour tissues. (a) and (b) The immunoblotting sheet transferred from the SDS-PAGE gels is specifically stained for VEGFR-3, whose positive bands on the nitrocellulose strip are noted at approximately 70 and 130 kDa. Note the non-metastatic lymph node (a) shows extremely lower VEGFR-3 signals than the metastatic one (b). (c) RT-PCR expression patterns of mRNAs for LYVE-1, podoplanin, *Prox-1*, VEGFR-3 and vWF are shown in each panel separately with different molecular sizes of the amplified fragments. GAPDH is used as an internal control.

approximately 70 and 130 kDa, in which the non-metastatic lymph nodes showed extremely lower VEGFR-3 signals than the metastatic ones (Figure 8a,b). The high expression of LYVE-1, podoplanin, *Prox-1* and VEGFR-3 mRNAs was confirmed in the tumour tissues of lymph node, liver, skin, kidney and diaphragm. In the pylorus, the mRNA level was much lower in VEGFR-3 and *Prox-1* than in podoplanin and LYVE-1. The blood vascular marker vWF was differently expressed in these tumour tissues (Figure 8c).

Discussion

Lymphatics have many biological properties in comparison with blood vessels. The present study has shown that 5′-Nase-positive initial lymphatics with blind-ended structures are composed of a single endothelial layer, and represent a wide irregular lumen and obvious overlapping intercellular junctions. On the other hand, ALPase-positive blood vessels showed strong CD31 immunoreactivity and were usually accompanied by numerous lymphatics. It is generally accepted that the basement membrane of blood capillaries is developed with encircling pericytes and commonly existed tight junctions, whereas initial lymphatics lack mural cells and are characterized by an incomplete or absent basement membrane (Ji 2006b). The thin-walled initial lymphatics offer less resistance and more contact area for penetration of tumour cells into the lymphatic system than blood vessels, although a pre-existing blood vascular bed may be necessary to guide lymphangiogenesis. The lymphatic and blood vascular systems might be coordinately regulated by different molecules in their growth and development because they are functionally interconnected and act together to maintain fluid homeostasis in tissues and cell nutrition.

The abnormal function of lymphatics has been implicated in processes as diverse as lymphoedema, inflammation and tumours such as lymphangioma, and especially serves as a major route for tumour metastasis. Although tumours metastasize to lymph nodes via the lymphatics, the importance of intratumoural and peritumoural lymphangiogenesis or/and

pre-existing lymphatics in mediating the process remains controversial. Recently, the discovery of active tumour lymphangiogenesis and its role in tumour metastasis has drawn considerable attention to the molecular mechanisms that control activation and proliferation of LECs (Alitalo & Carmeliet 2002; Ji 2005), but the LEC expression of the functional molecules in ITLs or PTLs is still not well defined. The present study immunohistochemically demonstrated that podoplanin, LYVE-1 and VEGFR-3 are exclusively expressed on both the luminal and abluminal surfaces of lymphatics and that *Prox-1* is mainly distributed in LEC nucleus and up-regulated on vascular endothelial cells in several tumour-involved tissues. In combination with histochemical results, the Western blot and RT-PCR analysis have indicated a distinct profile of the protein and mRNA expression by LEC-specific markers in the hybridoma-induced tumour tissues. The mRNA expression of LYVE-1, podoplanin, *Prox-1* and VEGFR-3 is abundant in many tumour tissues, but in the pyloric tumour, the mRNA level is much lower in VEGFR-3 and *Prox-1* than in podoplanin and LYVE-1. This may reflect local variations of LEC proliferating potentials and tumour microenvironment such as differences in extracellular matrix composition (Skobe *et al.* 2001). On the basis of the present findings of different expression by these markers in the tumour tissues, we suppose that VEGFR-3 and *Prox-1* are mainly restricted to proliferating endothelial cells, whereas LYVE-1 and podoplanin are expressed by both developing and mature LECs. The extremely lower VEGFR-3 signal expression in the non-metastatic lymph nodes other than metastatic lymph nodes may suggest a strong lymphangiogenic activity in metastatic tissues. Moreover, the different mRNA expression by the endothelial marker vWF probably indicates a variable extent in the distribution of blood vessels within the tumour tissues (Mancardi *et al.* 1999). The comprehensive identification of lymphangiogenic signals reflecting LEC-specific functions may, in part, provide the molecular basis for the analysis of ITLs and PTLs, although the expression of tumour cells by podoplanin and *Prox-1* was also detected in this study. Therefore, it seems also necessary to evaluate the segregated LECs and blood endothelial cells from the hybridoma-induced tumour tissues *in vitro*.

ITLs contribute to tumour cell dissemination

Although ITLs have been proposed to be non-functional depending on the assays of microlymphangiography and interstitial fluid pressure in some tumour models (Padera *et al.* 2002), the presence of *de novo* intratumoural lymphangiogenesis and/or increased lymphatic vessel density should be regarded as an additional and important pathway for lymph node metastasis (Ji 2006b). The present findings have shown that ITLs randomly dispersed in close contact with tumour cells are the most direct route for lymphatic invasion. Noteworthily, ITLs have shown much wider area in the non-solid tumour tissues than in the solid tumour mass. The scattered and slender lymphatics offer a great feature in non-solid tumour tissues where malignant cells may take advantage of extensive extracellular space to penetrate the lymphatic walls. In the solid tumour, the collapse of ITLs may be due to mechanical stress and increased interstitial pressure generated by proliferating tumour cells (Jain & Fenton 2002). Although tumour cell density may exert a direct functional effect on ITLs, LECs and tumour cells are dependent upon the extracellular matrix for survival and proliferation. Increased ITL vessel density demonstrated in this study will provide a comprehensive tumour-endothelial interface and facilitate the access of tumour cells to the lymphatics. In primary human tumours, the univariate proportional hazard analysis has revealed that the presence of ITLs is a significant risk factor for the development of lymph node metastasis, suggesting an active role of lymphangiogenesis within the tumour parenchyma (Dadras *et al.* 2003). New proliferating LECs and increasing ITL vessel density should be used as a criterion to separate patients at higher risk of an adverse clinical outcome (Straume *et al.* 2003). The more the lymphatic vessels, the greater probability is that tumour cells invade the lymphatic bed and escape from the original site of tumours (Ji 2006b). However, the lymphatic 'functionality' is still a disputed issue, and arguments have given rise to the view that PTLs may be of a greater importance in lymph node metastases than ITLs.

PTLs mediate tumour cell spreading/implantation into the intraorganic parenchyma and regional lymph nodes

It has been suggested that PTLs are likely to be pre-existing lymphatics that have enlarged in response to VEGF-C rather than newly formed lymphatics. In human breast tumour, lymph node metastasis can sufficiently proceed via the pre-existing lymphatics (Williams *et al.* 2003), implying that lymphangiogenesis may not necessarily be involved at the tumour periphery regardless of ITL vessel density. However, peritumoural lymphangiogenesis stimulated by VEGF-A was recently documented in a murine xenograft tumour model (Bjorndahl *et al.* 2005). The new vessel growth sprouting from pre-existing limbal lymphatics at the tumour periphery via a VEGF-C/-D/VEGFR-3-independent pathway has promoted lymph node metastasis. Especially, less aggressive cancers may require newly formed lymphatics in peripheral tumours to disperse more cells and increase the probability

of dissemination. It has long been known that lymphatic endothelial walls are anchored to the extracellular matrix by fine filaments and show a morphological modification in the intercellular junctions that open as a response to an increase of interstitial fluid pressure, permitting the entry of fluid and particles into initial lymphatics. As the tissue pressure decreases, lymphatic valves close and prevent lymph backflow. Dysfunctional open junctions and valves will result in significant microcirculation impediment (Ji 2005). Our present study has confirmed that lymphatics at the invasive front of solid tumours are enlarged and perfused, whereas those in the central portions of the tumour are compressed, small and flattened. PTLs were usually filled with clusters of malignant cells and have abnormal twisty valves in the severe metastatic tumour tissues, suggesting that these collecting lymphatics may have some biological properties and play a key role in tumour progression (Ji 2006b). In consistent with our observation, functional lymphangiographic analysis of PTLs has displayed a retrograde draining pattern in VEGF-C-overexpressing tumours (Isaka *et al.* 2004), indicating a possible disorder of these lymphatic valves. Lymphatics induced by VEGF-C allow retrograde flow, potentially because the dysfunctional valves are unable to close properly and thus result in lateral flow into side lymphatics (Nagy *et al.* 2002). VEGF-C may thus induce new but immature lymphatics including those at the tumour periphery.

Lymphatic invasion may depend on lymphangiogenesis and pre-existing lymphatics

The early dissemination of malignant tumours via lymphatics to regional lymph nodes is one of the most important indicators of tumour aggressiveness. The metastasis requires tumour cell adhesion to LECs and transmigration into lymph nodes through the immatured or dysfunctional lymphatics. The tumour cell invasion into the lymphatics is established by the destruction of surrounding stroma via activation of matrix-digesting enzymes, which are produced by tumour cells or fibroblasts (Hofmann *et al.* 2003), and by the up-regulation of autocrine motility factor receptor expression on tumour cells (Hirono *et al.* 1996). Morphologically, it has been assumed that the intercellular junctions of newly formed lymphatics may provide a favourite site for transendothelial spread of tumour cells (Ji 2006b). The present finding that tumour cells with their metabolic products adhered to or penetrated slender endothelial walls also suggests that the identification of adhesion molecules typical for LECs may be particularly important for the understanding of leucocyte trafficking and tumour metastasis via lymphatics, especially their intercellular junctions.

Tumour cells have been proposed to invade and destroy the pre-existing lymphatics rather than promoting their proliferation. In the past few years, the application of several major players in the regulation of new lymphatic formation has provided direct experimental evidence that increased tumour lymphangiogenesis promotes regional lymph node metastasis in animal tumour models (Mandriota *et al.* 2001). The initial lymphatics appear to have remarkable capacity to sprouting, splitting, branching and differential growth and regeneration in the embryonic and differentiated tissues, and in some pathological events such as wound healing and aggressive tumours (Valencak *et al.* 2004; Ji 2005). Lymphangiogenic factors, e.g. VEGF-C/-D produced by tumour cells may induce proliferation and dilatation of PTLs, as well as proliferation of ITLs, thereby favouring the metastatic spread. The overexpression of VEGF-C/-D is associated with an increased number of functionally draining lymphatics and tumour cell dissemination (Jeltsch *et al.* 1997). The hyperplasia appears to result from both increased endothelial cell proliferation in the pre-existing lymphatics and the formation of additional lymphatics (Veikkola *et al.* 2001), although the biologic relevance of peritumoural and intratumoural lymphangiogenesis may vary depending on tumour cell density. Moreover, activation of LECs by VEGF-C/-D can promote release of chemokines, which attract tumour cells into the lymphatics. Different from VEGF-C/-D expression, the expression of a single chemokine receptor gene (CCR7) by murine melanoma cells also increases metastases to lymph nodes, in which tumour cells may probably use normal mechanisms of lymph node homing for metastatic dissemination (Muller *et al.* 2001). In our recent study, LECs were demonstrated to be up-regulated in adhesion molecules CD31 and CCL21 (the ligand of CCR7) chemokine in the non-obese diabetic mice (Ji *et al.* 2006). Firmly attached malignant tumour cells and other lymphocytes on endothelial cells may easily follow a chemotactic gradient into lymphatics or actively gain access into the lymphatic system by inducing intratumoural or peritumoural lymphangiogenesis and by co-opting pre-existing lymphatics (Ji 2006b).

In summary, no matter what kind of lymphatic-related disorders may be, a causative factor should be stressed on the endothelial cells of lymphatic networks. Clearly, an investigation into the current unsettled issue still remains the most invigorative and productive field that the phenotype and functional differences in molecular expression and ultrastructure exist between newly formed and pre-existing lymphatics in the tumour-involved tissues. The possibility of a close interconnection between ITLs and PTLs has indicated that the functional lymphatics either within the tumour

mass or at the tumour periphery are essential for lymph node metastasis and should be targeted therapeutically. Therefore, the hybridoma-induced tumour model is useful to study the morphology and localization of ITLs and PTLs, and to inquire into the interaction between tumour cells and lymphatics in multiple-organ carcinogenesis. We are now trying to apply this model to determine the effect of tumour-associated lymphatics on the individual organ with respect to the transport of fluids and macromolecules.

References

Achen M.G., McColl B.K., Stacker S.A. (2005) Focus on lymphangiogenesis in tumor metastasis. *Cancer Cell* **7**, 121–127.

Alitalo K. & Carmeliet P. (2002) Molecular mechanisms of lymphangiogenesis in health and disease. *Cancer Cell* **1**, 219–227.

Alitalo K., Tammela T., Petrova T.V. (2005) Lymphangiogenesis in development and human disease. *Nature* **438**, 946–953.

Beasley N.J., Prevo R., Banerji S. *et al.* (2002) Intratumoral lymphangiogenesis and lymph node metastasis in head and neck cancer. *Cancer Res.* **62**, 1315–1320.

Bjorndahl M.A., Cao R., Burton J.B. *et al.* (2005) Vascular endothelial growth factor-a promotes peritumoral lymphangiogenesis and lymphatic metastasis. *Cancer Res.* **65**, 9261–9268.

Breiteneder-Geleff S., Soleiman A., Kowalski H. *et al.* (1999) Angiosarcomas express mixed endothelial phenotypes of blood and lymphatic capillaries: podoplanin as a specific marker for lymphatic endothelium. *Am. J. Pathol.* **154**, 385–394.

Burke Z. & Oliver G. (2002) Prox1 is an early specific marker for the developing liver and pancreas in the mammalian foregut endoderm. *Mech. Dev.* **118**, 147–155.

Dadras S.S., Paul T., Bertoncini J. *et al.* (2003) Tumor lymphangiogenesis: a novel prognostic indicator for cutaneous melanoma metastasis and survival. *Am. J. Pathol.* **162**, 1951–1960.

Hirono Y., Fushida S., Yonemura Y., Yamamoto H., Watanabe H., Raz A. (1996) Expression of autocrine motility factor receptor correlates with disease progression in human gastric cancer. *Br. J. Cancer* **74**, 2003–2007.

Hofmann U.B., Eggert A.A., Blass K., Brocker E.B., Becker J.C. (2003) Expression of matrix metalloproteinases in the microenvironment of spontaneous and experimental melanoma metastases reflects the requirements for tumor formation. *Cancer Res.* **63**, 8221–8225.

Isaka N., Padera T.P., Hagendoorn J., Fukumura D., Jain R.K. (2004) Peritumor lymphatics induced by vascular endothelial growth factor-C exhibit abnormal function. *Cancer Res.* **64**, 4400–4404.

Jain R.K. & Fenton B.T. (2002) Intratumoral lymphatic vessels: a case of mistaken identity or malfunction? *J. Natl. Cancer Inst.* **94**, 417–421.

Jeltsch M., Kaipainen A., Joukov V. *et al.* (1997) Hyperplasia of lymphatic vessels in VEGF-C transgenic mice. *Science* **276**, 1423–1425.

Ji R.C. (2005) Characteristics of lymphatic endothelial cells in physiological and pathological conditions. *Histol. Histopathol.* **20**, 155–175.

Ji R.C. (2006a) Lymphatic endothelial cells, lymphangiogenesis, and extracellular matrix. *Lymphat. Res. Biol.* **4**, 83–100.

Ji R.C. (2006b) Lymphatic endothelial cells, tumor lymphangiogenesis and metastasis: new insights into intratumoral and peritumoral lymphatics. *Cancer Metastasis Rev.* **25**, 677–694.

Ji R.C., Qu P., Kato S. (2003) Application of a new 5′-nase monoclonal antibody specific for lymphatic endothelial cells. *Lab. Invest.* **83**, 1681–1683.

Ji R.C., Kurihara K., Kato S. (2006) Lymphatic vascular endothelial hyaluronan receptor (LYVE)-1- and CCL21-positive lymphatic compartments in the diabetic thymus. *Anat. Sci. Int.* **81**, 201–209.

Jussila L., Valtola R., Partanen T.A. *et al.* (1998) Lymphatic endothelium and Kaposi's sarcoma spindle cells detected by antibodies against the vascular endothelial growth factor receptor-3. *Cancer Res.* **58**, 1599–1604.

Kahn H.J., Bailey D., Marks A. (2002) Monoclonal antibody D2–40, a new marker of lymphatic endothelium, reacts with Kaposi's sarcoma and a subset of angiosarcomas. *Mod. Pathol.* **15**, 434–440.

Mancardi S., Stanta G., Dusetti N. *et al.* (1999) Lymphatic endothelial tumors induced by intraperitoneal injection of incomplete Freund's adjuvant. *Exp. Cell Res.* **246**, 368–375.

Mandriota S.J., Jussila L., Jeltsch M. *et al.* (2001) Vascular endothelial growth factor-C-mediated lymphangiogenesis promotes tumour metastasis. *EMBO J.* **20**, 672–682.

Morisada T., Oike Y., Yamada Y. *et al.* (2005) Angiopoietin-1 promotes LYVE-1-positive lymphatic vessel formation. *Blood* **105**, 4649–4656.

Mouta Carreira C., Nasser S.M., di Tomaso E. *et al.* (2001) LYVE-1 is not restricted to the lymph vessels: expression in normal liver blood sinusoids and down-regulation in human liver cancer and cirrhosis. *Cancer Res.* **61**, 8079–8084.

Muller A., Homey B., Soto H. *et al.* (2001) Involvement of chemokine receptors in breast cancer metastasis. *Nature* **410**, 50–56.

Nagy J.A., Vasile E., Feng D. *et al.* (2002) Vascular permeability factor/vascular endothelial growth factor induces lymphangiogenesis as well as angiogenesis. *J. Exp. Med.* **196**, 1497–1506.

Ordonez N.G. (2005) D2–40 and podoplanin are highly specific and sensitive immunohistochemical markers of epithelioid malignant mesothelioma. *Hum. Pathol.* **36**, 372–380.

Padera T.P., Kadambi A., di Tomaso E. *et al.* (2002) Lymphatic metastasis in the absence of functional intratumor lymphatics. *Science* **296**, 1883–1886.

Roy S., Chu A., Trojanowski J.Q., Zhang P.J. (2005) D2–40, a novel monoclonal antibody against the M2A antigen as a marker to distinguish hemangioblastomas from renal cell carcinomas. *Acta Neuropathol. (Berl.)* **109**, 497–502.

Schiwek D., Endlich N., Holzman L., Holthofer H., Kriz W., Endlich K. (2004) Stable expression of nephrin and localization to cell-cell contacts in novel murine podocyte cell lines. *Kidney Int.* **66**, 91–101.

Skobe M., Hawighorst T., Jackson D.G. *et al.* (2001) Induction of tumor lymphangiogenesis by VEGF-C promotes breast cancer metastasis. *Nat. Med.* **7**, 192–198.

Stacker S.A., Caesar C., Baldwin M.E. *et al.* (2001) VEGF-D promotes the metastatic spread of tumor cells via the lymphatics. *Nat. Med.* **7**, 186–191.

Straume O., Jackson D.G., Akslen L.A. (2003) Independent prognostic impact of lymphatic vessel density and presence of low-grade lymphangiogenesis in cutaneous melanoma. *Clin. Cancer Res.* **9**, 250–256.

Valencak J., Heere-Ress E., Kopp T., Schoppmann S.F., Kittler H., Pehamberger H. (2004) Selective immunohistochemical staining shows significant prognostic influence of lymphatic and blood vessels in patients with malignant melanoma. *Eur. J. Cancer.* **40**, 358–364.

Veikkola T., Jussila L., Makinen T. *et al.* (2001) Signalling via vascular endothelial growth factor receptor-3 is sufficient for lymphangiogenesis in transgenic mice. *EMBO J.* **20**, 1223–1231.

Williams C.S., Leek R.D., Robson A.M. *et al.* (2003) Absence of lymphangiogenesis and intratumoural lymph vessels in human metastatic breast cancer. *J. Pathol.* **200**, 195–206.